

WIND EFFECT ON THE PLASMA INSTABILITIES OPERATING IN THE MIDLATITUDE IONOSPHERIC E REGION

M. VOICULESCU,¹ M. IGNAT²

¹ Faculty of Sciences, “Dunărea de Jos” University, Galați, Romania
E-mail: Mirela.Voiculescu@ugal.ro

² Faculty of Physics, “Al. I. Cuza” University, Iași, Romania
E-mail: emignat@uaic.ro

(Received July 15, 2005)

Abstract. Two types of instabilities act to generate ondulatory phenomena in the midlatitude ionospheric E region plasma: the gradient-drift and the modified two stream instabilities. We review here the physical mechanisms, the dispersion relation and the growth rate of the two instabilities, and discuss the wind role in producing meter-scale waves in the midlatitude E region. The wind has not been included in the study of the E region instabilities, which are usually connected only with the electric field. We show that for normal propagation the wind shear does not modify the amplification of the wave, but has important effects on the growth rate when the wave vector deviates from the normal. On the other hand, at the macroscopic level, the wind favours or hinders the generation of the waves. Our results prove that the wind reduces significantly the electric fields values required for the generation of both types of waves, especially for the very rarely observed Farley-Bunemann waves.

Key words: gradient-drift instability, Farley-Bunemann instability, midlatitude ionospheric plasma, small-scale ionospheric waves.

1. INTRODUCTION

The existence of plasma waves in the E region is known for several decades [1–4]. The wavelength range covers a very large domain but we focus here on the meter-scale irregularities. These waves are electrostatic and only the electric field is perturbed, while the magnetic field is unaffected [1]. In the midlatitude E region they originate from two instability mechanisms: the gradient drift instability – GD (or the cross – field instability) and the FB instability (or the modified two stream instability) [1, 2].

The ionospheric irregularities are investigated using HF and VHF coherent scatter radars [2, 3]. The observations of backscatter echoes have shown that the plasma waves propagate coherently parallel with the geomagnetic field lines. Due

to the large difference between the parallel and transversal mobility of the electrons, the diffusion of plasma normally to the field lines is strongly inhibited. Consequently, the irregularities have practically only a longitudinal component and their wave vector, \mathbf{k} , is very close to the normal to the field lines [4–7]. The magnetic aspect angle, α , is the angle between the wave vector and a direction normal to \mathbf{B} . The wave fronts are almost parallel to the magnetic field lines ($k_p \ll k_\perp$) so that the meter scale plasma irregularities observed in the E region are known as FAI (Filed Aligned Irregularities).

Using several simplifying assumptions, the dispersion relationship was studied by [8] while the development of the linear theory in non-local approximation can be found in [9]. However, these authors have stated that ion contribution should be minor to the instability development, but this contribution has not been quantified. We will present in this paper the calculus of the dispersion relationship of the two instabilities known to occur in the midlatitude E region, the gradient drift and Farley Bunemann instabilities, taken into consideration a vertical wind shear. In order to find these relations we will make several simplifying assumptions, sustained however by the experimental observations. We will discuss the conditions when its contribution should be considered. We also present an analysis of the E region wind and electric field values which are required to set off the two instabilities.

2. DISPERSION EQUATION

The ionospheric plasma is a cold plasma, because the temperature and the geomagnetic field values are such that the thermal energy density is small relatively to the magnetic energy [1]:

$$\frac{k_B N(T_e + T_i)}{\frac{B^2}{2\mu_0}} \ll 1.$$

For the waves whose wavelength is greater than 1 m the fluid approximation can be used [1]. Also, the condition of quasineutrality is valid and we start from the continuity and momentum equation for electrons ($s = e$) and ions ($s = i$). As long as the wave amplitudes remain small enough, the linear approximation can be applied to calculate the frequency and growth rate of the waves [8, 10]. The plasma dynamics at E region heights depends on the values of the so-called *mobility coefficient*, which is the ratio of the gyrofrequency to the collision frequency:

$$\beta_{e,i} = \frac{\Omega_{e,i}}{\nu_{e,i}}.$$

The E region plasma is dominated by the collisions with the neutrals, which are several orders of magnitude denser than the plasma components. For the ions the collision frequency varies rapidly with height relatively to their gyrofrequency, which is about 100 s^{-1} . The ion-neutral collision frequency decreases from 10^4 s^{-1} at 90 km to 10 s^{-1} at 140 km. The electrons collide much often with neutrals but at these altitudes their collision frequency remains 100–1000 times smaller than the gyrofrequency. Practically, the electrons are unaffected by the winds and move almost freely along the geomagnetic field lines when an electric field acts upon them, while the ions are unmagnetized and their movement is governed by neutrals.

The continuity equation, in fluid approximation, is:

$$\frac{\partial N_1}{\partial t} + \nabla \cdot (N_1 \mathbf{V}_{s1}) = 0, \quad (1)$$

while the momentum equations are:

$$m_s \frac{d\mathbf{V}_{s1}}{dt} = e (-\nabla \phi + \mathbf{V}_{s1} \times \mathbf{B}) - \nabla p_s - m_s v_s (\mathbf{V}_{s1} - \mathbf{U}). \quad (2)$$

The equilibrium velocity of ions and electrons is given by equation (2), where for the E region $\beta_i < 1 < \beta_e$ and $\beta_i^2 \ll 1 \ll \beta_e$. The values of the other coefficients are: $\frac{K_B T_e}{m_e v_e N} \cong 10^{-4}$ and $\frac{e}{m_e v_e} = \frac{\beta_e}{B}$. Under these circumstances and in a geographic coordinate system with x towards East, y to North and z upwards, the macroscopic electron velocity is:

$$\mathbf{V}_{e0} = \mathbf{U}_p - \frac{K_B T_e}{m_e v_e N} \beta_e^2 (\nabla N)_n - \beta_e \mathbf{E}_p - \frac{1}{\beta_e} \frac{\mathbf{E}}{B} + \frac{\mathbf{E} \times \mathbf{B}}{B^2} \quad (3)$$

where \mathbf{U}_p and \mathbf{E}_p are the wind and electric field which are parallel to the geomagnetic field lines. The ion velocity is:

$$\mathbf{V}_{i0} = \mathbf{U} + \beta_i \frac{\mathbf{E}}{B} + \beta_i (\mathbf{U} \times \mathbf{b}) \quad (4)$$

Each perturbed quantity can be written:

$$F_1 = F + \delta f,$$

where F is the unperturbed quantity, $(N, \mathbf{V}_e, \mathbf{V}_i, \phi)$ and δf is the linear perturbation:

$$\delta f = f e^{i(\omega t - \mathbf{k} \cdot \mathbf{r})} = f e^{i(\omega t - k_x x - k_y y)}$$

Other assumptions are:

- The electron inertial effects are negligible.
- The wind has a zonal component (U_x).

– The electron velocity can be perturbed in any directions, while for the ion the propagation is restricted only in the x direction. This assumption is justified also by the fact that in the lower E region the ions are practically unmagnetized:

$$\begin{aligned}\mathbf{v}_e &= (v_{ex}, v_{ey}, v_{ez}), \\ \mathbf{v}_i &= (v_{ix}, 0, 0).\end{aligned}$$

– The neutral wind varies with the altitude and the vertical shear is described by:

$$\frac{dU_z}{dz} = w_s \neq 0. \quad (5)$$

– The density gradient is vertical:

$$\nabla N = \left(0, 0, \frac{dN}{dz} \right).$$

– The gradient scale length is introduced as:

$$L = N \left(\frac{dN}{dz} \right)^{-1}. \quad (6)$$

The linearly perturbed equations are projected on the three axes of the coordinate system so that a system of equations is obtained:

$$-(\omega - \mathbf{k} \cdot \mathbf{V}_e) \frac{n}{N} + k_x v_{ex} + k_y v_{ey} + i \frac{v_{ez}}{L} = 0, \quad (7)$$

$$-(\omega - \mathbf{k} \cdot \mathbf{V}_i - i w_s) \frac{n}{N} + k_x v_{ix} = 0 \quad (8)$$

$$i k_x \frac{K_B T_e}{m_e} \frac{n}{N} - \frac{i k_x e}{m_e} \phi + \Omega_e v_{ey} \sin I + \Omega_e v_{ez} \cos I - v_e v_{ex} = 0, \quad (9)$$

$$i k_y \frac{K_B T_e}{m_e} \frac{n}{N} - \frac{i k_y e}{m_e} \phi - \Omega_e \sin I v_{ex} - v_e v_{ey} = 0, \quad (10)$$

$$- \Omega_e v_{ex} \cos I - v_e v_{ez} = 0, \quad (11)$$

$$\left[i(\omega - \mathbf{k} \cdot \mathbf{V}_i) + v_i \right] v_{ix} - i k_x \frac{K_B T_i}{m_i} \frac{n}{N} - i \frac{k_x e}{m_i} \phi = 0. \quad (12)$$

Because the calculations are very laborious, we will present only some intermediate steps. In order to simplify the calculus, we note $P_e = \mathbf{k} \cdot \mathbf{V}_e - \omega$, $P_i = \mathbf{k} \cdot \mathbf{V}_i - \omega$, $S = \sin I$, $C = \cos I$. The unknowns, v_{ex} , v_{ey} , v_{ez} , v_{ix} , ϕ and n/N , will be found if:

$$\begin{aligned}
& -\frac{i}{L} k_x \Omega_e^2 S C \frac{k_x k_y k_B}{m_i} (T_e + T_i) - \frac{i}{L} k_x^3 v_e \Omega_e C \frac{k_B (T_e + T_i)}{m_i} + \\
& + \Omega_e^2 C^2 k_x^2 k_y^2 \frac{k_B (T_e + T_i)}{m_i} - i k_x^2 \Omega_e^2 v_e C^2 \frac{m_e}{m_i} P_e + \\
& + k_x^2 v_e \left[\Omega_e S \frac{k_x k_y k_B}{m_i} (T_e + T_i) + \frac{v_e k_x^2 k_B}{m_i} (T_e + T_i) \right] + \\
& + k_x v_e^2 \left[\frac{k_x k_y^2 k_B}{m_i} (T_e + T_i) - i v_e \frac{k_x m_i}{m_e} P_e \right] - \\
& - k_x v_e \Omega_e S \left[i \Omega_e S k_x \frac{m_e}{m_i} P_e + \frac{k_x^2 k_y k_B}{m_i} (T_e + T_i) \right] - i (P_i + i w_s) (-i P_i + v_i) \times \\
& \times \left(k_x^2 v_e^2 - k_x \Omega_e v_e C \frac{i}{L} + \Omega_e^2 C^2 k_y^2 - \Omega_e^2 S C k_y \frac{i}{L} + v_e^2 k_y^2 \right) = 0.
\end{aligned} \tag{13}$$

We note

$$\Psi_0 = \frac{v_e v_i}{\Omega_e \Omega_i}, \tag{14}$$

and observe that $\frac{m_e}{m_i} = \frac{\Omega_i}{\Omega_e}$. The ion acoustic velocity is $C_s^2 = \frac{k_B (T_e + T_i)}{m_i}$ whose variation with the altitude is shown in Fig. 1.

$$\begin{aligned}
\omega - \mathbf{k} \cdot \mathbf{V}_e &= -\frac{\Psi_0}{v_i} \left[-\frac{i}{L} \left(\frac{\Omega_e^2}{v_e^2} \sin I \cos I \frac{k_y}{k_x^2} + \frac{\Omega_e}{v_e} \cos I \frac{1}{k_x} \right) + \right. \\
& \left. + \frac{\Omega_e^2}{v_e^2} \cos^2 I \frac{k_y^2}{k_x^2} + \frac{k^2}{k_x^2} \right] \times \\
& \times \left[(\mathbf{k} \cdot \mathbf{V}_i - \omega + i w_s) (i \mathbf{k} \cdot \mathbf{V}_i - i \omega - v_i) - i k_x^2 C_s^2 \right].
\end{aligned} \tag{15}$$

Other notations are introduced:

$$\Psi = \Psi_0 \left(\frac{k^2}{k_x^2} + \frac{\Omega_e^2}{v_e^2} \frac{k_y^2}{k_x^2} \cos^2 I \right) = \Psi_0 (1 + \beta_e^2 \sin^2 \alpha), \tag{16}$$

$$G_L = \frac{\Omega_e}{v_e} \frac{k_y}{k_x} \sin I \cos I + \cos I = \beta_e \sin I \sin \alpha + \cos I, \tag{17}$$

Taking into consideration that $\beta_e^2 \gg 1$, we can write now:

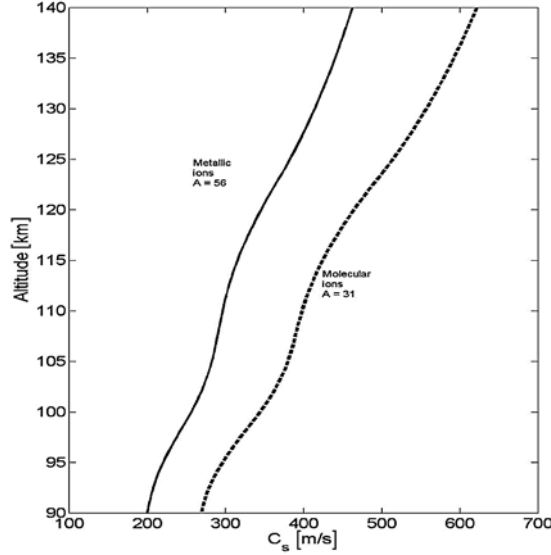


Fig. 1 – Variation of the ion acoustic velocity with altitude (due to the temperature variation).

$$\omega - \mathbf{k} \cdot \mathbf{V}_e = \left(-\frac{iG_L}{k_x L \Omega_i} + \frac{\Psi}{v_i} \right) \times \quad (18)$$

$$\times \left[(\omega - \mathbf{k} \cdot \mathbf{V}_i - i w_s)(i \mathbf{k} \cdot \mathbf{V}_i - i \omega - v_i) + i k_x^2 C_s^2 \right].$$

The real and imaginary parts of ω are the angular frequency, ω_r , and the growth rate, γ , $\omega = \omega_r + i\gamma$, which splits equation (18) into two parts:

$$\omega_r - \mathbf{k} \cdot \mathbf{V}_e = -(\omega_r - \mathbf{k} \cdot \mathbf{V}_i)^2 \frac{G_L}{k_x \Omega_i L} - \frac{\Psi}{v_i} (\omega_r - \mathbf{k} \cdot \mathbf{V}_i)(2\gamma + v_i + \omega_s) + \quad (19)$$

$$+ \frac{G_L}{k_x \Omega_i L} (\gamma + w_s)(\gamma + v_i) + k_x^2 C_s^2 \frac{G_L}{k_x \Omega_i L},$$

and:

$$\gamma = (\omega_r - \mathbf{k} \cdot \mathbf{V}_i)^2 \frac{\Psi}{v_i} - (\omega_r - \mathbf{k} \cdot \mathbf{V}_i) \frac{G_L}{k_x \Omega_i L} (2\gamma + v_i + \omega_s) - \quad (20)$$

$$- (\gamma + w_s)(\gamma + v_i) \frac{\Psi}{v_i} - k_x^2 C_s^2 \frac{\Psi}{v_i}.$$

First, we evaluate the growth rate. Because of the linear approximation, $\gamma \ll \omega_r$ and $\gamma \ll v_i$:

$$\gamma = \frac{1}{(1+\Psi)} \left\{ \frac{\Psi}{v_i} \left[(\omega_r - \mathbf{k} \cdot \mathbf{V}_i)^2 - k_x^2 C_s^2 + w_s v_i \right] - (\omega_r - \mathbf{k} \cdot \mathbf{V}_i) \frac{G_L v_i}{k_x \Omega_i L} \right\}. \quad (21)$$

Due to the geomagnetic field, the propagation of waves is not isotropic. The components of the wave vector in the two directions, parallel and normal to the geomagnetic lines, are:

$$k_p^2 = k_y^2 \cos^2 I, \quad k_\perp^2 = k_y^2 \sin^2 I + k_x^2. \quad (22)$$

After introducing the wave vector components and replacing G_L , the growth rate of the unstable waves is:

$$\begin{aligned} \gamma = \frac{1}{(1+\psi)} \left\{ \frac{\psi}{v_i} \left[(\omega_r - \mathbf{k} \cdot \mathbf{V}_i)^2 - (k_\perp^2 - k_p^2 \operatorname{tg}^2 I) C_s^2 + w_s v_i \right] - \right. \\ \left. - (\omega_r - \mathbf{k} \cdot \mathbf{V}_i) \frac{v_i \cos I}{(k_\perp^2 - k_p^2 \operatorname{tg}^2 I)^{\frac{1}{2}} \Omega_i L} \times \right. \\ \left. \times \left(\frac{\Omega_e}{v_e} k_p \sin I + (k_\perp^2 - k_p^2 \operatorname{tg}^2 I)^{\frac{1}{2}} \right) \right\}. \quad (23) \end{aligned}$$

The wave frequency (19) will be:

$$\begin{aligned} \omega_r - \mathbf{k} \cdot \mathbf{V}_e = -\psi (\omega_r - \mathbf{k} \cdot \mathbf{V}_i) \left(\frac{2\gamma}{v_i} + \frac{\omega_s}{v_i} + 1 \right) + \\ + \frac{G_L v_i}{k_x \Omega_i L} \left[\frac{-(\omega_r - \mathbf{k} \cdot \mathbf{V}_i)^2 + k_x^2 C_s^2}{v_i} + \frac{\gamma^2}{v_i} + \gamma + \frac{\omega_s \gamma}{v_i} + w_s \right]. \quad (24) \end{aligned}$$

which, in linear approximation is:

$$\begin{aligned} \omega_r - \frac{\mathbf{k} \cdot (\mathbf{V}_e + \psi \mathbf{V}_i)}{(1+\psi)} = \frac{G_L v_i}{k_x \Omega_i L} \frac{1}{1+\psi} \times \\ \times \left\{ -\frac{1}{v_i} \left[(\omega_r - \mathbf{k} \cdot \mathbf{V}_i)^2 - k_x^2 C_s^2 \right] + \gamma + w_s \right\}. \quad (25) \end{aligned}$$

Using (23), we obtain:

$$\omega_r - \frac{\mathbf{k} \cdot (\mathbf{V}_e + \psi \mathbf{V}_i)}{(1+\psi)} = \frac{G_L v_i}{k_x \Omega_i L} \frac{1}{1+\psi} \left\{ -(\omega_r - \mathbf{k} \cdot \mathbf{V}_i) \frac{G_L v_i}{k_x \Omega_i L} \frac{1}{1+\psi} + \gamma \right\}. \quad (26)$$

The RTS of (26) can be neglected if [9]:

$$\frac{G_L v_i}{k \Omega_i} \frac{1}{(1+\psi)} \ll L,$$

i.e., only when the wavelength is small enough compared to the gradient scale length, which practically is called the local approximation of the dispersion relation-

ship of the instabilities. For normal propagation and for a gradient scale of 100 m (exceptionally small and associated only with very abrupt variations of the plasma density), this theory will be valid for wavelengths whose value is between 1 and λ_{\max} :

$$\lambda \ll \lambda_{\max} = \frac{2\pi\Omega_i L(1+\psi)}{v_i \cos I}.$$

For parallel propagation $k_p \ll k_\perp$ and $k \cong k_x$, $\alpha \cong 0$, the dispersion relationship is:

$$\omega_r = \frac{\mathbf{k} \cdot (\mathbf{V}_e + \psi \mathbf{V}_i)}{1 + \psi}, \quad (27)$$

and the growth rate:

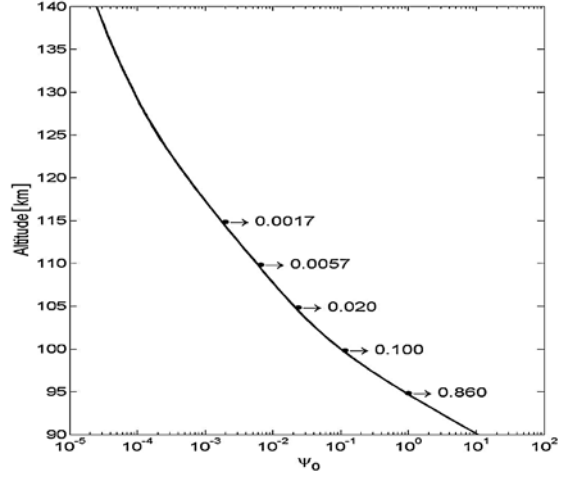
$$\gamma = \frac{\psi}{(1+\psi)v_i} \left[\frac{(\mathbf{k} \cdot \mathbf{V}_d)^2}{(1+\psi)^2} - k^2 C_s^2 \right] - \frac{\mathbf{k} \cdot \mathbf{V}_d}{(1+\psi)^2} \frac{v_i \cos I}{\Omega_i L k} - \frac{w_s \psi}{1+\psi}. \quad (28)$$

The first term corresponds to the growth of the waves caused by the Farley Bunemann instability, while the third one is associated with the gradient drift instability. The waves cannot grow ad infinitum due the diffusion, described by the second term. The last term is the contribution of the shear, which is important when ψ is large. This happens for $\alpha > 0$ or at low altitudes. A small deviation, of 0.5 degrees, from parallel propagation is sufficiently great to produce considerable effects due to the $\beta_e^2 \sin^2 \alpha$ component of ψ . A very small departure from the field alignment, of 0.01 degrees, results in a dramatic decrease of the propagation velocity and of the growth rate. This means that for propagation which is not parallel to the field lines the wind shear stops the growth of the waves.

3. DISCUSSION

The dispersion relationship (27) is identical with what [10] or [11] have found in the absence of wind. The growth rate, on the other hand, contains a new term, $-w_s \psi / (1 + \psi)$, which represent the wind shear. At altitudes of 100–105 km the wind shear could be $w_s = 0.1\text{--}0.5 \text{ s}^{-1}$. Keeping in mind that the values of ψ_0 vary from 0.5 at 95 km to 0.005 at 110 km (Fig. 2), the contribution of the shear to the growth rate decreases from 0.1 to about 0,01. Such values are not significant for growth rates of 5–10 s. Conversely, when the irregularities propagate on a direction that deviates from the field line, even with a small angle, the value of ψ is modified and the contribution of the wind-shear could be higher than any other term. In this paper we will analyse the wave propagation whose wavevector is normal to the field lines.

Fig. 2 – Values of the ψ_0 coefficient in the E region.



The phase velocity is:

$$V_f = \frac{\omega}{k} = \frac{\mathbf{k}}{k} \cdot \left[\frac{\mathbf{V}_d}{(1 + \psi_0)} + \mathbf{V}_i \right]. \quad (29)$$

If the ions are at rest or if the process is studied in a neutral coordinate system, $\mathbf{V}_d = \mathbf{V}_e$ and ω_r is positive when $\mathbf{k} \cdot \mathbf{V}_e > 0$, which means that the wave propagates in the same sense as the electrons. For normal propagation, $\alpha = 0$ and $\psi = \psi_0$.

The growth rate is [10]:

$$\gamma = \frac{\psi_0}{(1 + \psi_0)v_i} \left[\frac{(\mathbf{k} \cdot \mathbf{V}_d)^2}{(1 + \psi_0)^2} - k^2 C_s^2 \right] + \frac{\mathbf{k} \cdot \mathbf{V}_d}{(1 + \psi_0)^2} \cdot \frac{v_i}{\Omega_i L_{eff} k}, \quad (30)$$

where $\mathbf{V}_d = \mathbf{V}_e - \mathbf{V}_i$ is the drift velocity of electrons relatively to the ions and L_{eff} is the gradient scale length is the general case (regardless of the coordinate system):

$$L_{eff} = \frac{k N_0 B}{\mathbf{k}_\perp \cdot (\nabla \mathbf{N} \times \mathbf{B})} \mathbb{k}. \quad (31)$$

This shows that the evolution of the irregularities depends on the orientation of the wave vector and of the density gradient relatively to the geomagnetic field. Note that L and L_{eff} have opposite signs; L introduced in (4) is in fact the particular case of L_{eff} for horizontal propagation. The majority of authors prefer to work in coordinate system attached to the ions (although this could be misleading when the neutral wind is important). In such a coordinate system the phase velocity is:

$$V_f = \frac{\omega}{k} = \frac{\mathbf{k}}{k} \cdot \frac{\mathbf{V}_e}{(1 + \psi_0)} = \frac{\mathbf{k}}{k} \cdot \frac{\mathbf{V}_d}{(1 + \psi_0)}, \tag{32}$$

which shows that the instability develops only if $\mathbf{k} \cdot \mathbf{V}_d > 0$. This means that the density gradient is destabilizing only if its orientation is such as \mathbf{k}_\perp and $(\nabla N \times \mathbf{B})$ have the same direction.

In a geographic system, the above considerations are applicable for altitudes higher than 105 km, where ψ_0 is smaller than 0.01. For lower altitudes, between 90 and 105 km, when ψ_0 approaches 1, the wave progress is less clear. At midlatitudes the electric field is generally small, thus electrons have small velocities (20–30 m/s), while the neutral drag can drive the ions to 50–100 m/s. In this case the propagation direction will be along $\mathbf{V}_e + \psi_0 \mathbf{V}_i$. A higher electric field (higher than 5 mV for instance), reduces the effect of the ion dynamics on the phase velocity of the meter scale irregularities. A neutral wind has a higher importance on growth rate, because of the $\mathbf{k} \cdot \mathbf{V}_i$ term in (30). The increase or decrease of the wave depends significantly of the directions and magnitude of the two main factors at midlatitude, the wind and the electric field.

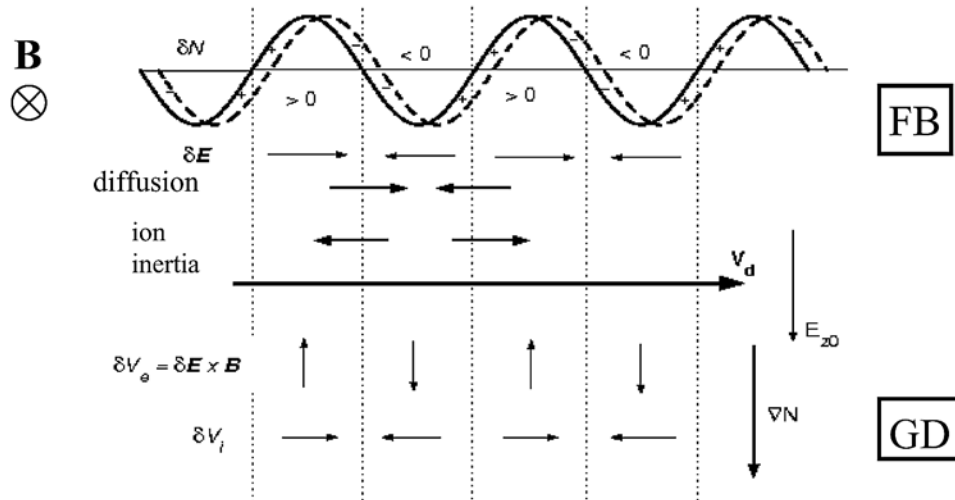


Fig. 3 – The schematic mechanisms of the Farley Bunemann (up) and gradient drift (down) instabilities. (adaptation after [1, 2]). The geomagnetic field (B) is normal to the page.

3.1. THE FARLEY BUNEMANN INSTABILITY

For small wavelengths and normal density gradients (gradient scale length greater than 2 km), the growth rate is dominated by the first term:

$$\gamma_{FB} \cong \frac{\psi_0}{(1 + \psi_0)v_i} \left[\frac{(\mathbf{k} \cdot \mathbf{V}_d)^2}{(1 + \psi_0)^2} - k^2 C_s^2 \right]. \quad (33)$$

When $\mathbf{k} \cdot \mathbf{V}_d \geq k C_s (1 + \psi_0)$, the electron stream relatively to the ions is supersonic and the modified two stream instability is triggered (known also as the Farley-Bunemann instability [12]). If the drift direction is inclined relatively to the wave vector with an angle which is smaller than a given θ , the marginal drift is:

$$V_{dimFB} \cos \theta \geq C_s (1 + \psi_0).$$

The electron velocity relatively to the ions must be higher than C_s , which is between 200–400 m/s (depending of the latitude). Physically this means that the ion inertia cancels the ion diffusion effect (described by the second term) which would result in the attenuation of the density. The growth rate for different conditions is shown in Fig. 4.

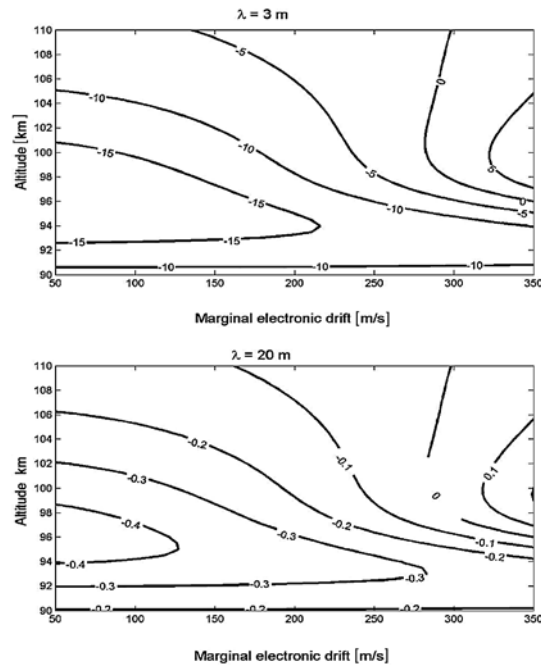


Fig. 4 – The growth rate of the FB instability: a) for 3 m waves (corresponding to 50 MHz); b) for 20-m waves (15 MHz).

The plots show clearly that the wave growth is favoured at low altitudes and the FB instability is responsible for waves whose wavelength is smaller than 10 m. The waves propagate in the meridional and zonal directions, transversal to the geomagnetic field. The marginal electronic drifts in the E region should be: (see (5) and (6), where $\beta_i \ll 1$ și $\beta_e \gg 1$):

$$\begin{aligned}
 V_{dx} &= V_{ex} - V_{ix} = \frac{E_y}{B} \sin I - U_x \geq C_s(1 + \psi_0) \\
 V_{dy} &= V_{ey} - V_{iy} = \frac{E_x}{B} - U_y \cos I \geq C_s(1 + \psi_0)
 \end{aligned}
 \tag{34}$$

where E_x and E_y are the zonal and meridional components of the electric field and U_x and U_y the meridional and zonal winds.

The electric field that could produce the FB waves can be found from Fig. 5. The altitude range where the FB instability could work is very small due to the rapid variation of ψ with the altitude. In other words, the instability acts on the plasma fluctuations at those points where both C_s and ψ_0 are relatively small, *i.e.* between 100 and 105 km. On the other hand, the electric fields at midlatitudes are 0,5–2 mV/m, thus the FB waves are extremely improbable. Indeed, the backscatter echoes on FAI at 9 MHz, 15 MHz, 25 MHz, 50 MHz show that only 2% of the echoes could be associated to the FB instability at midlatitudes [3, 4, 13–16].

The presence of the FB waves at midlatitudes, shown for the first time by [7] is interpreted as an indicator of extreme values of the electric fields (15–20 mV/m) [16, 17]. There is no experimental evidence of such electric fields at midlatitudes. Moreover, the polarisation mechanisms proposed to explain these observations resulted also in lower values for the electric field [18]. Fig. 5 shows that this is not necessary true. Our results suggest that neglecting the neutral dynamics and

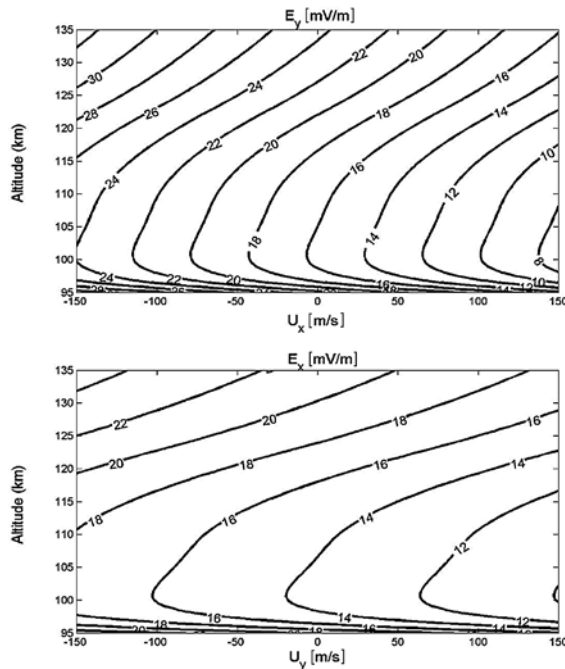


Fig. 5 – The electric fields required for the generation of the 3-m ionospheric waves by the Farley Bunemann instability
a) meridionally; b) zonally.

considering only the electron velocity is misleading. The electrons dynamics is important only relatively to the ions, which follow practically the neutrals. Fig. 5 proves clearly that the electric field are not necessarily extremely high and lower values 10–12 mV/m are enough to excite the FB mode when the wind reaches 150 m/s. These wind speeds are not extreme and are also experimentally confirmed by [19], who have measured them especially in regions where sporadic E layers exist.

In conclusion, the rarely observed FB waves could be explained by a high (but not improbable) electric field coexisting with an appropriate wind.

2.2. THE GRADIENT-DRIFT INSTABILITY

For decameter-waves (wavelengths of tens of meters) the attenuation due to diffusion is weaker (due to the k^2 dependence). If the gradient scale length is small (*i.e.* for high density gradients), the third term must be considered:

$$\gamma_{GD} = -\frac{\mathbf{k} \cdot \mathbf{V}_d}{(1 + \psi_0)^2} \frac{v_i}{\Omega_i L k} \cos I - \frac{\psi_0 k^2 C_s^2}{(1 + \psi_0) v_i}. \quad (35)$$

This is the growth rate associated to the gradient-drift mechanism (see Fig. 3). The marginal stability condition for FAI ($\gamma = 0$) implies that the marginal drift (the lowest velocity which can produce the instability) is [2, 10, 20]:

$$\mathbf{k} \cdot \mathbf{V}_{\text{dimGD}} = k C_s (1 + \psi_0) \left(\sqrt{F^2 + 1} - F \right), \quad (36)$$

where:

$$F = \frac{v_i^2}{2 \Omega_i k^2 C_s L_{ef} \psi_0}. \quad (37)$$

The wave grows when if L and $\mathbf{k} \cdot \mathbf{V}_d$ have opposite signs. The perturbations will propagate towards north and/or East (positive sense of the coordinate system) only if dN/dz and \mathbf{V}_d are antiparalel. The behavior of the plasma waves when the density gradients are medium or high can be described looking at Figs. 6–8. A relative electronic drift with an eastward component destabilizes the plasma when the plasma density decreases with the altitude. An opposite drift will generate GD plasma waves propagating to East in an altitude range hare the plasma density increases fast with the altitude. Generally, the GD instability amplifies the thermal plasma fluctuations if $\mathbf{k} \cdot \mathbf{V}_d$ and $\mathbf{k}_\perp \cdot (\nabla N \times \mathbf{B})$ are either positive or negative. In other words, waves propagate in the positive directions if $\mathbf{k}_\perp \cdot (\nabla N \times \mathbf{B})$ is positive. A westward drift generates waves if $\nabla N \times \mathbf{B}$ is also westward.

For instance, in the case of transversal propagation of waves generated by a perpendicular drift, the growth rate of the GD instability and the phase velocity of the waves are given by (32) and the marginal drift can be found using (36). If the

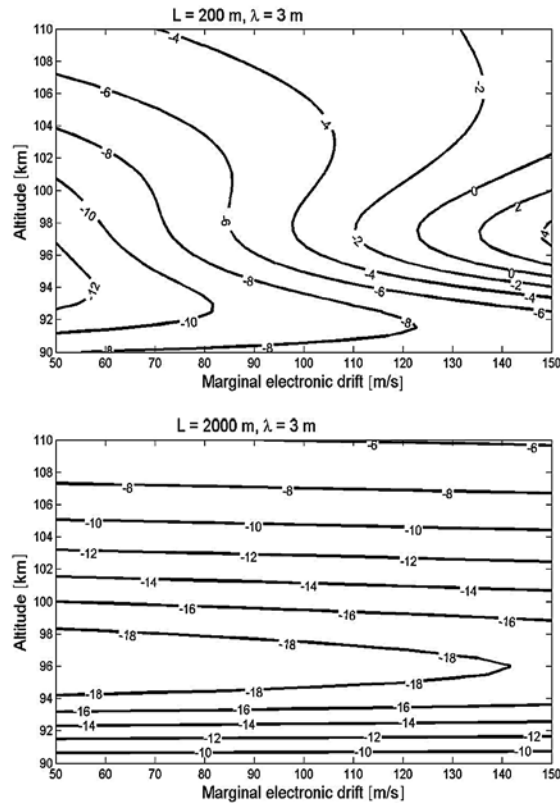


Fig. 6 – The growth rate of the 3m waves by the GD instability in the low E region where the FB instability could be produced.

plasma density is constant, which means $L_{eff} \rightarrow \infty$, thus $F = 0$, only the FB instability can be triggered. If $L_{eff} < 0$, the velocity which could initiate the unstable mode is too high, $V_{dimGD} > V_{dimFB}$ so that if the electrons move sufficiently fast the plasma fluctuations will be amplified by the FB instability. Only when L_{eff} is positive and small the GD instability is effective at midlatitudes. Fig. 8 shows the variation of the electron-ion drift with the altitude for different gradient scale lengths and for 3-m and, respectively, 10-m waves. The GD instability is favoured in the low E region and, in normal conditions, is effective for lower frequency waves. In a medium where the gradient scale length is 1000 m, a 3-m wave will develop if the electron-ion drift is about 250 m/s, while a 10-m wave could grow if the velocity is significantly smaller, 80–90 m/s. A high frequency wave requires a faster electron stream relatively to ions. If the neutrals are at rest (no wind) an electric field of 2 mV/m moves the electrons with about 45 m/s relatively to ions. Only decameter waves could be excited in this case, even if the plasma density varies abruptly. An opposite ion movement of 50 m/s, resulted from the action of a similar wind, small scale waves could develop on the horizontal walls of thin and dense sporadic E layers, which are often met in the midlatitude E region.

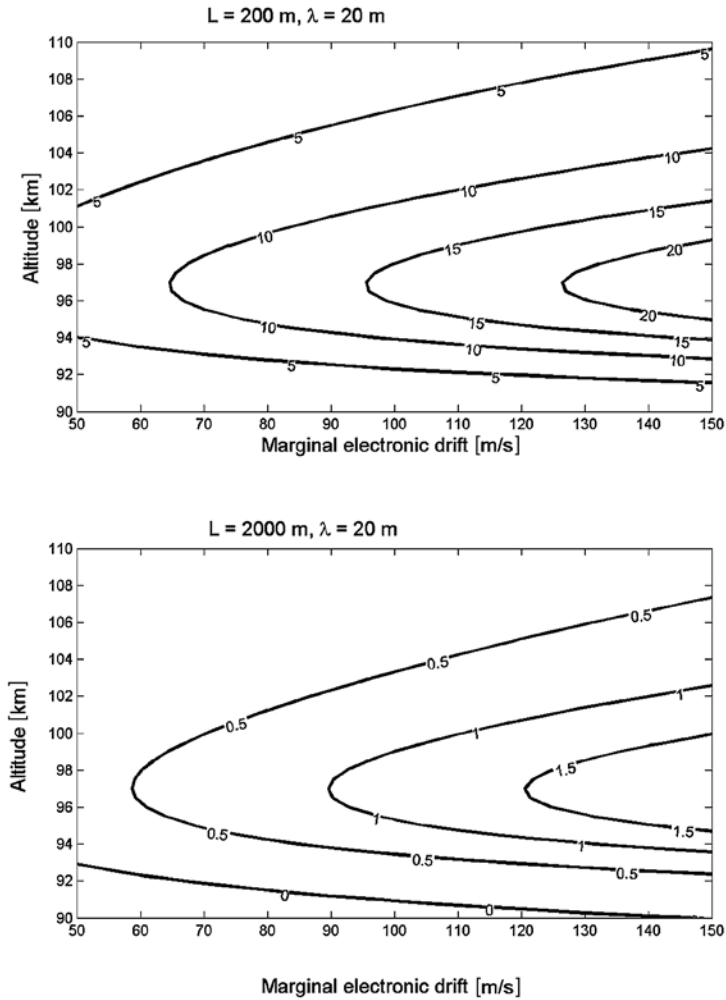


Fig. 7 – The growth rate for decameter waves ($\lambda = 20$ m), the effect of the existence of a differential drift of electrons relative to the ions (V_d) together with a density gradient (represented by its scale length L).

On the other hand, the marginal velocities decrease when the density gradient increases (smaller L). This happens on the walls of a sporadic E layer, where the density varies abruptly with height. The sporadic E layers are thin horizontal plasma layers where the density is one or two orders of magnitude higher than the background. They are observed in an altitude range of 95–125 km, have a lifetime of 30 minutes up to several hours and have vertical thickness of 1–5 km. The area of Es observation extends from low latitudes to high and even polar latitudes. Their characteristics and observation rate vary with the latitudinal range but they also have some common properties. The measurements have shown that they are composed

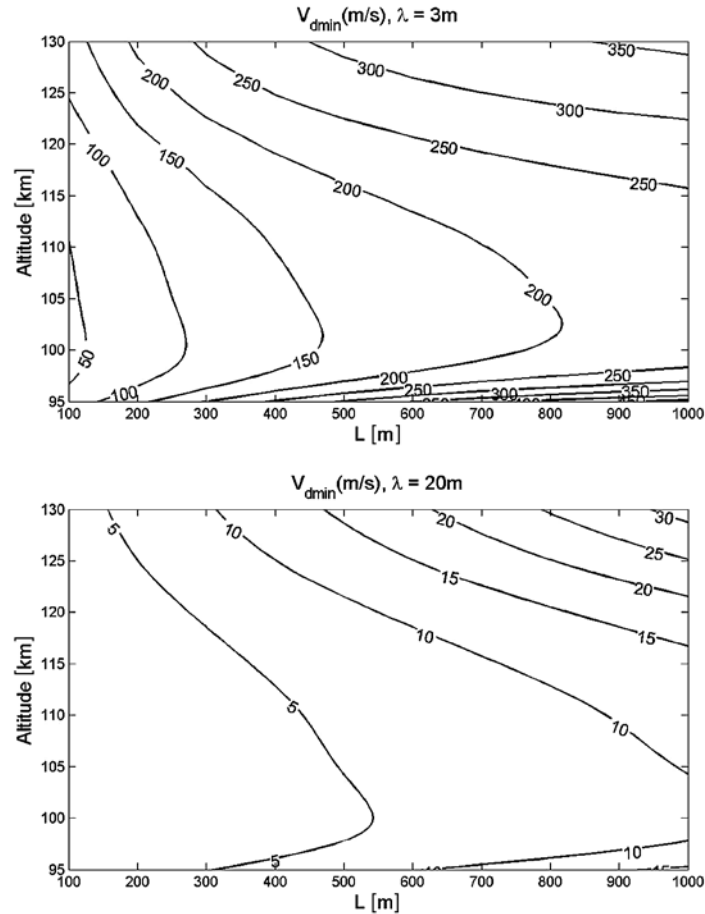


Fig. 8 – The marginal drifts for meter (a) and decameter (b) waves amplified by the GD instability for a) high gradients and b) normal gradients.

of metallic ions whose concentration reaches sometimes 80% of the positive plasma component. In such a case, the unstable GD mode amplifies the plasma fluctuation even for lower drifts. The waves propagate in a direction imposed by the orientation of the density gradient (up or down). For L values normally present in the E region, the marginal velocities are so high that the probability of the GD instability excitation is very low (5 km). When an Es layer is present, E_s , L can reach 500 m or even lower values, so that V_{dlimGD} is significantly smaller. Moreover, Fig. 1 suggests that the ion acoustic velocity, C_s , is reduced in an Es layer due to the presence of metallic ions. Consequently, the effect of diffusion is reduced [21] and both FB and GD instabilities are favoured.

The lower part of the Es layer, where L is positive in a geographic coordinate system, is destabilizing if the electrons move westwards faster than the ions (32).

A northward electric field, which will set up a Hall motion of the electrons, or a strong Eastward wind that would push the ions oppositely to west, can generate such a drift. Similarly, the upper part of the layer will set off eastward propagating waves in the presence of a southward electric field and/or a westward wind. Observations have shown that the density gradient is higher at the top of the Es layer than at the bottom, so the westward propagating FAI should dominate the coherent backscatter spectra. This is experimentally confirmed by [3], [4] and [14]. Also, the backscatter echoes are indeed very well correlated with the presence of Es layer [22, 23].

CONCLUSIONS

Two plasma instabilities act in the midlatitude E region to destabilize the ionospheric plasma; they are known as the gradient-drift and the Farley-Bunemann instabilities. At midlatitudes the second one is observed only for a very limited time (2–5% of observed radar spectra are connected with the Farley Bunemann instability). The waves are observed to propagate normally to the geomagnetic field lines. The dispersion relationship and the growth rate of these two instabilities are known but only in the presence of the electric field and ignoring the wind. In this view, the observation of Farley-Bunemann waves at midlatitudes was explained by the existence of very high electric fields which are almost impossible to exist at midlatitudes.

We have included the wind and its shear in deriving the dispersion relationship and the growth rate and analyse what are the effects on the propagation and development of both type of waves. We show that a wind-shear modifies the growth rate of the waves but has no effect on the dispersion relationship. On the other hand, at macroscopic scales, our results indicate that the wind reduces significantly the values of the electric field that were believed to produce the Farley Bunemann waves. These new values are still abnormally high for the E region, which explains why these waves are very rarely observed; however, such values have been measured or theoretically could develop in sporadic E layers. We also show that for waves whose propagation deviates with a very small angle from the normal, the wind-shear becomes a very important factor which should be considered in the analysis of the echoes spectra observed with coherent backscatter radars at midlatitudes.

REFERENCES

1. M. C. Kelley, *The Earth ionosphere: Plasma Physics and Electrodynamics*, Academic Press, New York, 1989.
2. B. G. Fejer. and M. C. Kelley, Ionospheric Irregularities, *Rev. Geophys and Space Phys.*, 18, 401, 1980.

3. T. Tanaka, and V. Venkateswaran, Characteristics of field-aligned E-region irregularities over Iioka (36°N), Japan – I, *J. Atmos. Terr Phys.*, *44*, 381, 1982a.
4. T. Tanaka, and V. Venkateswaran, Characteristics of field-aligned E-region irregularities over Iioka (36°N), Japan – II, *J. Atmos. Terr Phys.*, *44*, 395, 1982b.
5. K., Schlegel, Coherent backscatter from ionospheric E-region plasma irregularities, *J. Atmos. Terr. Phys.*, *58*, 933, 1996.
6. M. S. Yamamoto, S. Fukao, T. Ogawa, T. Tsuda, and S. Kato, A morphological study in midlatitude E-region field aligned irregularities observed with the MU radar, *J. Atmos. Terr. Phys.*, *54*, 769, 1992.
7. K. Schlegel, and C. Haldoupis, Observation of the modified two-stream instability in the midlatitude E region ionosphere, *J. Geophys. Res.*, *99*(A4), 6219, 1994.
8. R. N. Sudan, Unified theory of type I and type II irregularities in the equatorial electrojet, *J. Geophys. Res.*, *88*(6), 1983.
9. D. Riggis, and A. Kadish, Nonlocal theory of long wavelength plasma waves associated with sporadic E layers, *J. Geophys. Res.* *94*(A2), 1495, 1989.
10. B. G. Fejer, J. F. Providakes, and D. T. Farley, Theory of plasma waves in the auroral E region, *J. Geophys. Res.*, *89*, 7487, 1984.
11. R. N. Sudan, J. Akinrimisi, and D. T. Farley, Generation of small-scale field aligned irregularities in the equatorial electrojet, *J. Geophys. Res.*, *78*, 240, 1973.
12. D. T. Farley, A plasma instability resulting in field aligned irregularities in the ionosphere, *J. Geophys. Res.*, *68*, 6083, 1963.
13. M. S. Yamamoto, S. Fukao, R. F. Woodman, T. Ogawa, T. Tsuda, and S. Kato, Mid latitude E-region field aligned irregularities observed with the MU radar, *J. Geophys. Res.*, *96*, 15943, 1991.
14. A. Bourdillon, C. Haldoupis, and J. Delloue, High frequency Doppler radar observations of magnetic aspect sensitive irregularities on the midlatitude E region ionosphere, *J. Geophys. Res.* *100*, 21503, 1995.
15. C. Haldoupis, A. Kamboureli, K. Schlegel, and M. Voiculescu, First 50 MHz continuous wave interferometry measurements of localized backscatter regions in the midlatitude E region ionosphere, *Proceedings of the IUGG99 General Assembly*, Birmingham, 18-31.07. 1999a.
16. D. L. Hysell, and J. D. Burcham, The 30 MHz radar interferometer studies of midlatitude E region irregularities, *J. Geophys. Res.*, *105*, 2000.
17. C. Haldoupis, D. T. Farley, and K. Schlegel, Type-I echoes from the mid-latitude E-region ionosphere, *Ann. Geophys.*, *15*, 908, 1997.
18. S. Shalimov, C. Haldoupis and K. Schlegel, Large polarization electric fields associated with midlatitude sporadic E, *J. Geophys. Res.*, *103*(A6), 11617, **1998**.
19. M. F. Larsen, S. Fukao, M. Yamamoto, R. T. Tsunoda, K. Igarashi, and T. Ono, The SEEK chemical release experiment: Observed neutral wind profile in OH CCD images during the SEEK campaign, *Geophys. Res. Lett.*, *25*, 1793, 1998.
20. B. G. Fejer, Natural Ionospheric Plasma Waves, in *Modern Ionospheric Science*, (H. Kohl, R. Ruster, and K. Schlegel-editors) Katlenburg-Lindau, 1996.
22. K. Schlegel, The influence of metallic ions on the plasma instabilities in the high-latitude E-region, *Radio Sci.*, *20*, 740, 1985.
22. M. Voiculescu, C. Haldoupis, and K. Schlegel, Evidence for planetary wave effects on midlatitude backscatter and sporadic E layer occurrence, *Geophys. Res. Lett.*, *26*, 1105, 1999.
23. M. Voiculescu, C. Haldoupis, D. Pancheva, M. Ignat, K. Schlegel, and S. Shalimov, More evidence for a planetary wave link with midlatitude E region coherent back scatter and sporadic E layers, *Ann. Geophys.*, *18*, 1182, 2000.